

Vapor–Liquid Equilibrium in the Binary Systems 2-Butanol + *tert*-Amyl Methyl Ether, 2-Butanol + Heptane, and Heptane + *tert*-Amyl Methyl Ether

Andrés Mejía,* Hugo Segura,* and Marcela Cartes

Departamento de Ingeniería Química, Universidad de Concepción, POB 160-C, Correo 3, Concepción, Chile

S Supporting Information

ABSTRACT: Consistent vapor–liquid equilibrium (VLE) data have been measured for the systems 2-butanol + *tert*-amyl methyl ether (TAME), 2-butanol + heptane, and heptane + *tert*-amyl methyl ether at (50, 75, and 94) kPa. Equilibrium determinations were performed in a VLE still with circulation of both phases. According to experimental results, binary mixtures composed by 2-butanol exhibit positive deviations from ideal behavior, and azeotropy is present over the whole range of experimental determinations. The *n*-heptane + *tert*-amyl methyl ether binary system, in turn, exhibits slight positive deviation from ideal behavior, and no azeotrope is present. The VLE data of the quoted binary mixtures were well-correlated using the Redlich–Kister, Wohl, nonrandom two-liquid (NRTL), Wilson, and universal quasichemical (UNIQUAC) equations.

INTRODUCTION

During these last twenty years—once alkyl-lead and other metal-containing additives were phased out from commercial fuels—the rational formulation of new gasoline mixtures less harmful to the environment has been the focus of continuous and active research. Since then, significant improvements have been obtained in reducing carbon monoxide and partially burned hydrocarbon emissions by considering branched ethers (e.g., methyl-*tert*-butyl ether or MTBE, ethyl *tert*-butyl ether or ETBE, *tert*-amyl methyl ether or TAME, 2,2'-oxybis[propane] or DIPE) and alcohols (e.g., methanol, ethanol, butanol).¹ However, new challenges have also arisen as a consequence of the introduction of these mixtures in the dynamic transportation fuels market, namely: (a) potential human health hazards,² (b) inherent environmental risks that stem from fuel distribution, particularly soil³ pollution, air pollution,⁴ and contamination of aquifers,⁵ and (c) new technological concerns related to the efficient operation of internal combustion engines, since the reduced energy density of oxygenated fuels results in changes on combustion kinetics,⁶ in increased fuel consumption,⁷ and fears of damage to older technology-based cars.⁸ Mixtures of alcohols and ethers have been recently proposed as co-oxygenates in gasoline blending to strategically exploit their synergistic volatilities.⁹ Main advantages of these co-oxygenated gasoline mixtures are their effective octane enhancing capability, their flexible capability for meeting RVP (Reid vapor pressure) seasonal specifications, and additionally, some economical benefits directly associated to the industrial production of ethers. In fact, ethers can be synthesized from the dehydration of alcohols or more efficiently from isolefins with alcohol in surplus.¹⁰

To evaluate the performance of the quoted mixtures as fuel additives, as well as to optimize the separation processes and technological operations involved in ether's production, accurate vapor–liquid equilibrium (VLE) data are needed. Thermophysical properties of TAME based mixtures have not been broadly

characterized^{11,12} possibly due to its low RVP and low octane number. However, co-oxygenated mixtures of alcohol + TAME may potentially be used in gasoline blending to regulate fuel volatility.

Partial to complete VLE data have been previously reported for each one of the mixtures measured in this work, either at isothermal or isobaric conditions. For the case of 2-butanol + *n*-heptane, isobaric VLE data have been reported at 95 kPa by Vittal Prasad et al.¹³ and at 101.3 kPa by Yamamoto and Maruyama,¹⁴ Zong and Zheng,¹⁵ and Sabarathinam and Andiappan.¹⁶ Isothermal VLE data have also been reported over the temperature range (298.15 to 363.15) K by Pierotti et al.,¹⁷ Powell et al.,¹⁸ and Kumar and Katti.^{19,20} According to these experimental results, the system 2-butanol + *n*-heptane exhibits positive deviation from ideal behavior, and azeotropic behavior is present over the whole temperature and pressure range. For the case of 2-butanol + TAME, positive azeotropy has been reported over the temperature range (331.3 to 359.15) K by Gmehling and Bölts¹² and Evans and Edlund,²¹ while zeotropic behavior was detected at 12.90 kPa by Gmehling and Bölts.¹² Finally, VLE data for *n*-heptane + TAME mixture have been reported at (298.15 and 309.15) K by Moessner et al.²² and at 313.15 K by Chamorro et al.²³ and Kammerer et al.²⁴ According to the reported data, the system *n*-heptane + TAME exhibits a slight positive deviation from ideal behavior.

As part of our ongoing work devoted to experimental determinations of VLE of oxygenate additives to gasoline mixtures (see for instances refs 25 to 31) and since available experimental information for the entitled mixtures is incomplete or scarce, this contribution is devoted to reporting additional VLE experimental results for each one of the binary mixtures at three different pressure levels ((50, 75, and 94) kPa).

Received: November 24, 2010

Accepted: February 12, 2011

Published: February 28, 2011

Table 1. Gas Chromatography (GC) Purities (Mass Fraction), Refractive Index (n_D) at the Na D Line, Densities (ρ), and Normal Boiling Points (T_b)

component (purity/mass fraction)	n_D		$\rho / \text{g} \cdot \text{cm}^{-3}$		T_b / K	
	$T / \text{K} = 298.15$		$T / \text{K} = 298.15$		$p / \text{kPa} = 101.33$	
	exp.	lit. ^a	exp.	lit. ^a	exp.	lit. ^a
2-butanol (0.9997)	1.39676	1.39490	0.802985	0.80561	372.65	372.70
<i>n</i> -heptane (0.9985)	1.38668	1.38510	0.679555	0.68155	371.50	371.58
TAME (0.9986)	1.38712	1.38590	0.765835	0.76587	359.52	359.51

^a Daubert and Danner.³²**Table 2. Experimental VLE Data for 2-Butanol (1) + *n*-Heptane (2) at $p = 50.00 \text{ kPa}$ ^a**

T / K	x_1	y_1	γ_1	γ_2	$-B_{ij} / \text{cm}^3 \cdot \text{mol}^{-1}$		
					11	22	12
354.91	1.000	1.000	1.000		1301		
351.68	0.961	0.837	0.993	3.926	1622	1748	1042
349.08	0.918	0.716	0.997	3.502	1686	1786	1062
347.05	0.867	0.627	1.012	3.047	1740	1816	1078
345.36	0.811	0.557	1.038	2.680	1786	1842	1092
344.33	0.757	0.513	1.073	2.378	1815	1858	1100
343.57	0.708	0.479	1.112	2.165	1837	1870	1106
343.02	0.656	0.453	1.164	1.968	1853	1879	1111
342.54	0.611	0.432	1.218	1.837	1868	1887	1115
342.28	0.564	0.414	1.282	1.704	1876	1891	1117
342.04	0.516	0.399	1.367	1.588	1883	1895	1119
341.87	0.471	0.386	1.458	1.495	1888	1898	1121
341.74	0.421	0.371	1.581	1.403	1892	1900	1122
341.75	0.370	0.357	1.729	1.319	1892	1900	1122
341.67	0.322	0.342	1.911	1.256	1894	1901	1122
341.82	0.267	0.324	2.177	1.186	1890	1899	1121
341.91	0.218	0.307	2.517	1.136	1887	1897	1120
342.20	0.164	0.282	3.036	1.089	1878	1892	1118
342.62	0.114	0.252	3.824	1.055	1866	1886	1114
344.19	0.061	0.196	5.163	1.013	1819	1861	1101
349.24	0.000	0.000		1.000		1827	

^a T is equilibrium temperature, and x_i and y_i are mole fractions in liquid and vapor phase of component i , respectively. γ_i are activity coefficients of component i , and B_{ij} are molar virial coefficients.

EXPERIMENTAL SECTION

Purity of Materials. 2-Butanol (99.97+ mass %) and *n*-heptane (99.85+ mass %) were purchased from Merck and were used without further purification. TAME was purchased from Aldrich and then was further purified to 99.85+ mass % by rectification in a 1 m height and 30 mm diameter Normschliffgerätebau adiabatic distillation column (packed with $3 \times 3 \text{ mm}$ stainless steel spirals), working at a 1:100 reflux ratio. The properties and purity of the pure components, as determined by gas chromatography (GC), appear in Table 1. The densities and refractive indexes of pure liquids were measured at 298.15 K using an Anton Paar DMA 5000 densimeter (Austria) and a multiscale automatic refractometer RFM 81 (Bellingham &

Table 3. Experimental VLE Data for 2-Butanol (1) + *n*-Heptane (2) at $p = 75.00 \text{ kPa}$ ^a

T / K	x_1	y_1	γ_1	γ_2	$-B_{ij} / \text{cm}^3 \cdot \text{mol}^{-1}$		
					11	22	12
364.80	1.000	1.000	1.000		1189		
361.92	0.961	0.856	0.992	3.734	1402	1611	968
359.53	0.916	0.746	0.998	3.257	1448	1642	985
357.62	0.867	0.661	1.010	2.902	1488	1667	998
356.05	0.809	0.592	1.035	2.554	1521	1688	1009
354.98	0.755	0.546	1.069	2.294	1545	1702	1017
354.16	0.705	0.512	1.112	2.099	1564	1713	1023
353.73	0.655	0.486	1.158	1.915	1573	1719	1026
353.19	0.608	0.464	1.219	1.785	1586	1727	1030
353.02	0.563	0.448	1.280	1.658	1590	1729	1032
352.77	0.518	0.431	1.353	1.563	1596	1733	1033
352.79	0.470	0.416	1.442	1.456	1595	1733	1033
352.80	0.417	0.400	1.559	1.360	1595	1732	1033
352.74	0.368	0.384	1.702	1.290	1596	1733	1034
352.81	0.320	0.367	1.873	1.226	1595	1732	1033
352.88	0.266	0.347	2.123	1.170	1593	1731	1033
353.10	0.215	0.327	2.452	1.119	1588	1728	1031
353.51	0.163	0.300	2.926	1.077	1578	1722	1028
354.29	0.111	0.264	3.649	1.040	1561	1712	1022
356.22	0.062	0.197	4.564	1.010	1518	1685	1008
361.66	0.000	0.000		1.000		1643	

^a T is equilibrium temperature, and x_i and y_i are mole fractions in liquid and vapor phase of component i , respectively. γ_i are activity coefficients of component i , and B_{ij} are molar virial coefficients.

Stanley, England), respectively. Temperature was controlled to $\pm 0.01 \text{ K}$ with a thermostatted bath. The uncertainties in density and refractive index measurements are $5 \cdot 10^{-6} \text{ g} \cdot \text{cm}^{-3}$ and $\pm 10^{-5}$, respectively. The experimental values of these properties and the boiling points are given in Table 1 together with those given in the literature.

Apparatus and Procedure. Vapor–Liquid–Equilibrium Cell. An all-glass VLE apparatus model 601, manufactured by Fischer Labor and Verfahrenstechnik (Germany), was used in the equilibrium determinations. In this circulation-method apparatus, the mixture is heated to its boiling point by a 250 W immersion heater. The vapor–liquid mixture flows through an extended contact line (Cottrell pump) that guarantees an intense phase exchange and then enters to a separation chamber whose

Table 4. Experimental VLE Data for 2-Butanol (1) + *n*-Heptane (2) at $p = 94.00$ kPa^a

T/K	x_1	y_1	γ_1	γ_2	$-B_{ij}/\text{cm}^3 \cdot \text{mol}^{-1}$		
					11	22	12
370.66	1.000	1.000	1.000		1129		
367.76	0.962	0.867	1.001	3.679	1297	1540	930
365.59	0.916	0.763	1.004	3.172	1334	1566	944
363.88	0.867	0.682	1.013	2.809	1365	1587	955
362.33	0.807	0.612	1.038	2.470	1394	1606	965
361.37	0.756	0.568	1.069	2.232	1412	1618	972
360.49	0.705	0.533	1.115	2.049	1429	1629	978
359.89	0.655	0.506	1.168	1.884	1441	1637	982
359.61	0.606	0.484	1.220	1.740	1447	1641	984
359.45	0.561	0.467	1.280	1.621	1450	1643	985
359.30	0.517	0.450	1.348	1.526	1453	1645	986
359.22	0.468	0.433	1.437	1.432	1455	1646	987
359.25	0.417	0.416	1.550	1.343	1454	1645	987
359.27	0.367	0.399	1.689	1.271	1454	1645	986
359.29	0.319	0.381	1.861	1.214	1453	1645	986
359.52	0.263	0.360	2.108	1.153	1449	1642	985
359.71	0.214	0.338	2.419	1.110	1445	1639	983
360.19	0.162	0.309	2.870	1.071	1435	1633	980
361.22	0.112	0.269	3.488	1.035	1415	1620	973
363.55	0.061	0.197	4.297	1.002	1371	1591	957
369.04	0.000	0.000		1.000		1547	

^a T is equilibrium temperature, and x_i and y_i are mole fractions in liquid and vapor phase of component i , respectively. γ_i are activity coefficients of component i , and B_{ij} are molar virial coefficients.

construction prevents an entrainment of liquid particles into the vapor phase. The separated gas and liquid phases are condensed and returned to a mixing chamber, where they are stirred by a magnetic stirrer, and returned again to the immersion heater. The temperature in the VLE still is determined with a Systemteknik S1224 digital temperature meter and a Pt 100 probe which was calibrated against the boiling temperature data of the pure fluids used in this work. The uncertainty is estimated as ± 0.02 K. The total pressure of the system is controlled by a vacuum pump capable of work under vacuum up to 0.25 kPa. The pressure is measured with a Fischer pressure transducer calibrated against an absolute mercury-in-glass manometer (22 mm diameter precision tubing with cathetometer reading); the overall uncertainty is estimated as ± 0.03 kPa.

On average, the system reaches equilibrium conditions after (2 to 3) h operation. The 1.0 μL samples taken by syringe after the system had achieved equilibrium were analyzed by gas chromatography on a Varian 3400 apparatus provided with a thermal conductivity detector and a Thermo Separation Products model SP4400 electronic integrator. The column was 3 m long and 0.3 cm in diameter, packed with SE-30. Column, injector, and detector temperatures were (353.15, 393.15, and 493.15) K, respectively, for heptane mixtures and (373.15, 413.15, and 493.15) K for 2-butanol + TAME. Good separation was achieved under these conditions, and calibration analyses were carried out to convert the peak area ratio to the mass composition of the sample. The pertinent polynomial fit of the calibration data had a correlation coefficient R^2 better than 0.99. At least three analyses were made of each sample. Concentration

Table 5. Experimental VLE Data for 2-Butanol (1) + TAME (3) at $p = 50.00$ kPa^a

T/K	x_1	y_1	γ_1	γ_3	$-B_{ij}/\text{cm}^3 \cdot \text{mol}^{-1}$		
					11	33	13
337.64	0.000	0.000		1.000		1669	
337.65	0.047	0.043	2.021	1.004	2025	1624	1073
337.79	0.086	0.072	1.828	1.011	2020	1623	1072
338.04	0.139	0.107	1.667	1.023	2011	1620	1070
338.29	0.191	0.138	1.545	1.043	2003	1616	1068
338.67	0.244	0.170	1.453	1.062	1990	1612	1065
339.11	0.303	0.201	1.355	1.093	1976	1607	1062
339.52	0.357	0.228	1.277	1.130	1962	1601	1058
340.12	0.404	0.255	1.226	1.152	1943	1594	1054
340.73	0.452	0.285	1.190	1.179	1924	1587	1049
341.57	0.515	0.323	1.132	1.230	1898	1577	1043
342.39	0.578	0.367	1.103	1.286	1872	1567	1036
343.23	0.623	0.399	1.072	1.329	1848	1558	1030
344.19	0.672	0.442	1.049	1.379	1819	1547	1023
345.06	0.715	0.481	1.031	1.436	1795	1537	1017
346.51	0.771	0.543	1.011	1.498	1754	1521	1006
347.82	0.815	0.603	1.000	1.553	1719	1506	997
349.17	0.859	0.671	0.994	1.618	1684	1492	987
350.74	0.903	0.753	0.991	1.688	1644	1475	977
352.40	0.945	0.849	0.993	1.751	1604	1458	965
355.12	1.000	1.000	1.000			1299	

^a T is equilibrium temperature, and x_i and y_i are mole fractions in liquid and vapor phase of component i , respectively. γ_i are activity coefficients of component i , and B_{ij} are molar virial coefficients.

measurements were accurate to better than ± 0.001 in mole fraction. The previous experimental procedure has been validated both binary and ternary experimental determination of VLE.^{25–31}

RESULTS AND DISCUSSION

Vapor–Liquid Equilibrium. The equilibrium temperature T , liquid-phase x , and vapor-phase y mole fraction measurements at $p = (50, 75, \text{ and } 94)$ kPa for the three binary systems are reported in Tables 2 to 10 and illustrated in Figures 1 to 3. Tables 2 to 10 also show the activity coefficients (γ_i) that were calculated from the following equation:³³

$$\ln \gamma_i = \ln \frac{y_i P}{x_i P_i^0} + \frac{(B_{ii} - V_i^L)(P - P_i^0)}{RT} + y_j^2 \frac{\delta_{ij} P}{RT} \quad (1)$$

where P is the total pressure and P_i^0 is the pure component vapor pressure. V_i^L is the liquid molar volume of component i , R is the universal gas constant, B_{ii} and B_{jj} are the second virial coefficients of the pure gases, B_{ij} is the cross second virial coefficient, and

$$\delta_{ij} = 2B_{ij} - B_{jj} - B_{ii} \quad (2)$$

According to eq 2, the standard state for calculating activity coefficients is the pure component at the pressure and temperature of the solution. Equation 2 is valid from low to moderate pressures, where the virial equation of state truncated after the second term is adequate for describing the vapor phase of the pure components and their mixtures and, additionally, the liquid

Table 6. Experimental VLE Data for 2-Butanol (1) + TAME (3) at $p = 75.00$ kPa^a

T/K	x_1	y_1	γ_1	γ_3	$-B_{ij}/\text{cm}^3 \cdot \text{mol}^{-1}$		
					11	33	13
349.73	0.000	0.000		1.000			1506
349.65	0.047	0.047	1.910	1.004	1672	1487	984
349.69	0.085	0.081	1.789	1.008	1671	1486	984
349.75	0.138	0.119	1.625	1.023	1669	1486	983
349.88	0.192	0.156	1.517	1.042	1666	1484	982
350.28	0.243	0.190	1.427	1.056	1656	1480	980
350.63	0.304	0.225	1.330	1.087	1647	1476	977
351.06	0.355	0.255	1.267	1.113	1637	1472	974
351.53	0.403	0.284	1.216	1.139	1625	1467	971
351.76	0.457	0.316	1.177	1.191	1620	1464	970
352.79	0.518	0.357	1.121	1.223	1595	1454	963
353.46	0.578	0.400	1.093	1.278	1579	1447	958
354.19	0.623	0.436	1.072	1.317	1563	1439	953
354.79	0.671	0.476	1.058	1.380	1549	1433	949
355.70	0.714	0.516	1.039	1.423	1529	1424	943
357.32	0.770	0.580	1.010	1.471	1494	1408	933
358.44	0.814	0.637	1.002	1.526	1471	1398	926
359.70	0.858	0.703	0.996	1.583	1445	1385	918
361.06	0.902	0.778	0.995	1.642	1418	1373	910
362.52	0.944	0.866	0.998	1.681	1390	1359	901
365.20	1.000	1.000	1.000		1184		

^a T is equilibrium temperature, and x_i and y_i are mole fractions in liquid and vapor phase of component i , respectively. γ_i are activity coefficients of component i , and B_{ij} are molar virial coefficients.

Table 7. Experimental VLE Data for 2-Butanol (1) + TAME (3) at $p = 94.00$ kPa^a

T/K	x_1	y_1	γ_1	γ_3	$-B_{ij}/\text{cm}^3 \cdot \text{mol}^{-1}$		
					11	33	13
356.92	0.000	0.000		1.000			1421
356.79	0.047	0.049	1.850	1.004	1505	1414	936
356.77	0.085	0.085	1.745	1.008	1506	1414	937
356.74	0.137	0.126	1.600	1.022	1507	1414	937
356.84	0.191	0.165	1.497	1.039	1504	1413	936
357.09	0.243	0.201	1.409	1.056	1499	1411	934
357.31	0.303	0.238	1.327	1.087	1494	1408	933
357.62	0.355	0.270	1.268	1.115	1488	1405	931
358.03	0.403	0.300	1.219	1.143	1479	1402	929
358.50	0.455	0.334	1.179	1.175	1470	1397	926
359.26	0.516	0.376	1.133	1.213	1454	1390	921
359.88	0.577	0.420	1.102	1.270	1442	1384	917
360.83	0.622	0.458	1.071	1.295	1423	1375	911
361.41	0.670	0.496	1.052	1.357	1411	1369	907
362.20	0.712	0.536	1.037	1.400	1396	1362	903
363.66	0.769	0.599	1.013	1.451	1369	1349	894
364.72	0.813	0.657	1.009	1.489	1350	1339	888
365.83	0.858	0.720	1.003	1.556	1330	1329	881
366.82	0.901	0.791	1.010	1.628	1313	1321	875
368.44	0.944	0.873	1.002	1.666	1285	1306	866
371.17	1.000	1.000	1.000		1126		

^a T is equilibrium temperature, and x_i and y_i are mole fractions in liquid and vapor phase of component i , respectively. γ_i are activity coefficients of component i , and B_{ij} are molar virial coefficients.

Table 8. Experimental VLE Data for *n*-Heptane (2) + TAME (3) at $p = 50.00$ kPa^a

T/K	x_2	y_2	γ_2	γ_2	$-B_{ij}/\text{cm}^3 \cdot \text{mol}^{-1}$		
					22	33	23
337.66	0.000	0.000		1.000			1669
338.02	0.057	0.044	1.139	1.001	1962	1620	1690
338.35	0.108	0.083	1.115	1.005	1957	1616	1685
338.73	0.157	0.120	1.093	1.007	1950	1611	1680
339.06	0.208	0.159	1.079	1.014	1944	1607	1675
339.44	0.258	0.196	1.066	1.019	1938	1602	1670
339.81	0.306	0.234	1.058	1.025	1932	1598	1665
340.25	0.360	0.277	1.044	1.036	1924	1593	1659
340.79	0.408	0.318	1.039	1.037	1915	1586	1652
341.31	0.458	0.361	1.032	1.044	1907	1580	1645
341.85	0.511	0.408	1.024	1.054	1898	1574	1638
342.28	0.555	0.444	1.012	1.071	1891	1569	1632
342.88	0.599	0.491	1.014	1.068	1881	1562	1624
343.45	0.645	0.537	1.010	1.077	1872	1555	1616
344.01	0.691	0.586	1.009	1.088	1863	1549	1609
344.74	0.737	0.638	1.004	1.094	1852	1540	1600
345.44	0.783	0.691	1.001	1.103	1841	1533	1591
346.23	0.834	0.755	0.999	1.116	1829	1524	1581
347.05	0.885	0.823	0.998	1.134	1816	1515	1571
349.19	1.000	1.000	1.000		1828		

^a T is equilibrium temperature, and x_i and y_i are mole fractions in liquid and vapor phase of component i , respectively. γ_i are activity coefficients of component i , and B_{ij} are molar virial coefficients.

Table 9. Experimental VLE Data for *n*-Heptane (2) + TAME (3) at $p = 75.00$ kPa^a

T/K	x_2	y_2	γ_2	γ_2	$-B_{ij}/\text{cm}^3 \cdot \text{mol}^{-1}$		
					22	33	23
349.80	0.000	0.000		1.000			1505
350.18	0.059	0.046	1.117	1.002	1770	1481	1533
350.49	0.109	0.084	1.097	1.007	1765	1478	1529
350.87	0.158	0.122	1.081	1.010	1760	1474	1524
351.23	0.208	0.161	1.071	1.015	1755	1470	1520
351.62	0.258	0.200	1.062	1.020	1749	1466	1516
352.01	0.307	0.238	1.048	1.028	1743	1462	1511
352.50	0.360	0.282	1.042	1.034	1737	1457	1505
352.97	0.408	0.323	1.037	1.039	1730	1452	1500
353.48	0.459	0.366	1.029	1.048	1723	1447	1494
353.98	0.511	0.412	1.023	1.060	1716	1442	1488
354.57	0.556	0.453	1.014	1.066	1708	1436	1482
355.02	0.600	0.497	1.016	1.075	1702	1431	1477
355.73	0.645	0.542	1.008	1.080	1692	1424	1469
356.20	0.691	0.592	1.012	1.091	1685	1419	1463
357.01	0.738	0.644	1.005	1.095	1675	1411	1454
357.71	0.783	0.697	1.002	1.104	1665	1405	1447
358.47	0.834	0.760	1.003	1.119	1655	1397	1439
359.34	0.885	0.826	1.000	1.142	1644	1389	1429
361.60	1.000	1.000	1.000		1644		

^a T is equilibrium temperature, and x_i and y_i are mole fractions in liquid and vapor phase of component i , respectively. γ_i are activity coefficients of component i , and B_{ij} are molar virial coefficients.

Table 10. Experimental VLE Data for *n*-Heptane (2) + TAME (3) at $p = 94.00$ kPa^a

T/K	x_2	y_2	γ_2	γ_3	$-B_{ij}/\text{cm}^3 \cdot \text{mol}^{-1}$		
					22	33	23
357.04	0.000	0.000		1.000			1420
357.39	0.059	0.046	1.108	1.003	1670	1408	1450
357.73	0.110	0.085	1.092	1.007	1665	1404	1447
358.11	0.158	0.123	1.079	1.010	1660	1401	1443
358.46	0.209	0.162	1.063	1.016	1655	1397	1439
358.86	0.259	0.203	1.059	1.021	1650	1394	1434
359.29	0.307	0.241	1.047	1.027	1645	1389	1430
359.80	0.361	0.286	1.041	1.032	1638	1385	1424
360.27	0.409	0.327	1.035	1.038	1632	1380	1419
360.78	0.459	0.370	1.028	1.046	1626	1375	1414
361.25	0.511	0.416	1.023	1.059	1620	1371	1409
361.78	0.557	0.458	1.016	1.069	1613	1366	1404
362.30	0.600	0.501	1.016	1.074	1606	1361	1398
363.01	0.646	0.544	1.003	1.088	1598	1355	1391
363.50	0.691	0.596	1.012	1.091	1592	1350	1386
364.31	0.738	0.647	1.003	1.100	1582	1343	1378
364.88	0.783	0.700	1.006	1.113	1575	1338	1372
365.80	0.835	0.763	1.002	1.125	1564	1330	1363
366.70	0.885	0.830	1.001	1.132	1553	1322	1354
368.98	1.000	1.000	1.000				1548

^a T is equilibrium temperature, and x_i and y_i are mole fractions in liquid and vapor phase of component i , respectively. γ_i are activity coefficients of component i , and B_{ij} are molar virial coefficients.

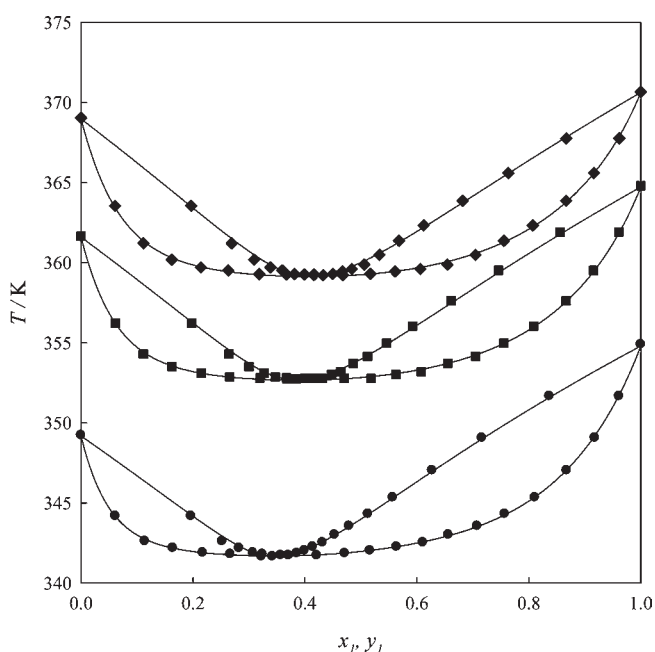


Figure 1. Isobaric phase diagrams for the system 2-butanol (1) + *n*-heptane (2). Experimental data at \bullet , 50.00 kPa; \blacksquare , 75.00 kPa; \blacklozenge , 94.00 kPa; —, as smoothed by the Wilson model, with parameters given in Table 15.

molar volumes of pure components are incompressible over the pressure range under consideration. Liquid molar volumes were estimated from the correlation proposed by Rackett.³⁴

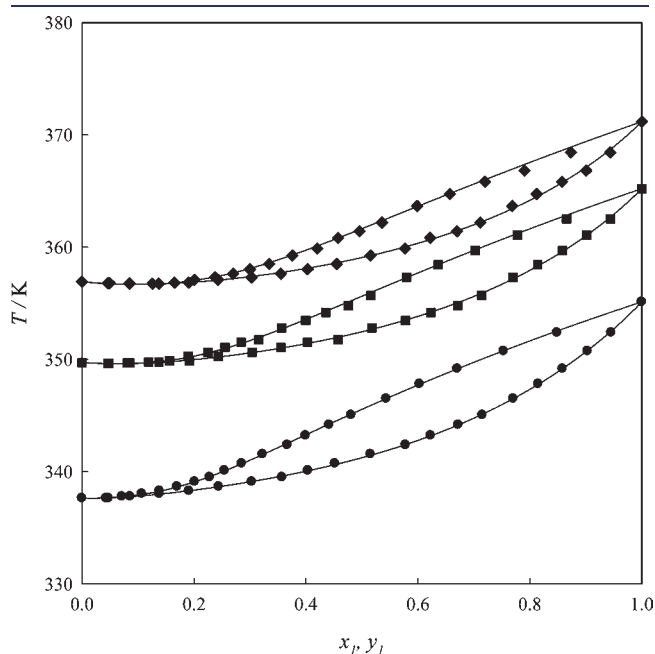


Figure 2. Isobaric phase diagrams for the system 2-butanol (1) + TAME (3). Experimental data at \bullet , 50.00 kPa; \blacksquare , 75.00 kPa; \blacklozenge , 94.00 kPa; —, as smoothed by the Wilson model, with parameters given in Table 16.

Table 11. Experimental Vapor Pressures (p) as a Function of Temperature (T) for Pure Fluids

2-butanol		<i>n</i> -heptane		TAME	
T/K	p/kPa	T/K	p/kPa	T/K	p/kPa
334.83	20.01	319.06	16.01	313.44	20.01
339.42	25.01	329.07	24.01	318.99	25.01
343.31	30.01	334.91	30.01	323.68	30.01
346.69	35.01	339.08	35.01	327.77	35.01
349.69	40.01	342.78	40.01	331.41	40.01
352.38	45.01	346.14	45.01	334.69	45.01
354.84	50.01	349.19	50.01	337.69	50.01
357.11	55.01	352.01	55.01	340.46	55.01
359.21	60.01	354.63	60.01	343.03	60.01
361.55	66.01	357.10	65.01	345.89	66.01
364.08	73.01	359.42	70.01	348.97	73.01
366.40	80.01	361.59	75.01	351.84	80.01
368.58	87.01	363.67	80.01	354.52	87.01
370.61	94.01	366.41	87.01	357.02	94.01
372.82	102.18	368.99	94.01	359.95	102.73
		371.63	101.74		

Table 12. Antoine Coefficients (A_i , B_i , and C_i) in eq 3

compound	A_i	B_i	C_i	temperature range/K
2-butanol	6.03018	1014.7635	-120.503	334.83 to 372.82
<i>n</i> -heptane	6.07980	1298.9367	-52.676	319.06 to 371.63
TAME	5.93073	1184.0871	-57.841	313.44 to 359.95

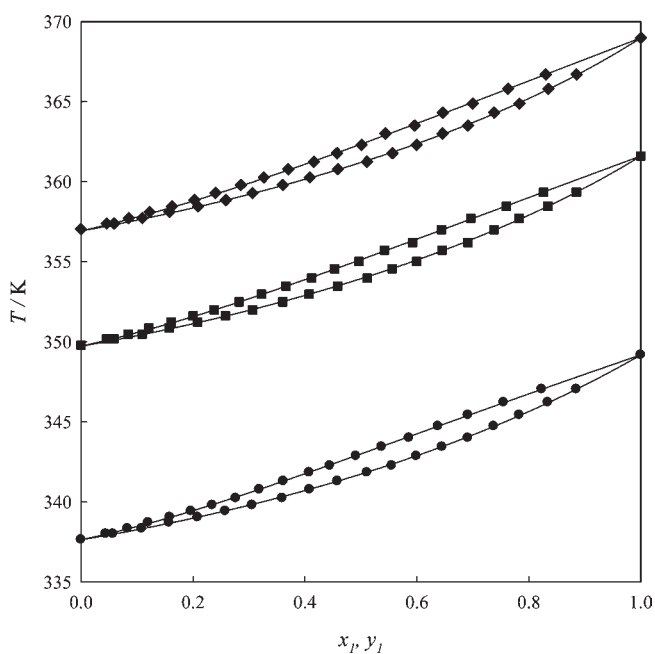


Figure 3. Isobaric phase diagrams for the system *n*-heptane (2) + TAME (3). Experimental data at ●, 50.00 kPa; ■, 75.00 kPa; ◆, 94.00 kPa; —, as smoothed by the Wilson model, with parameters given in Table 17.

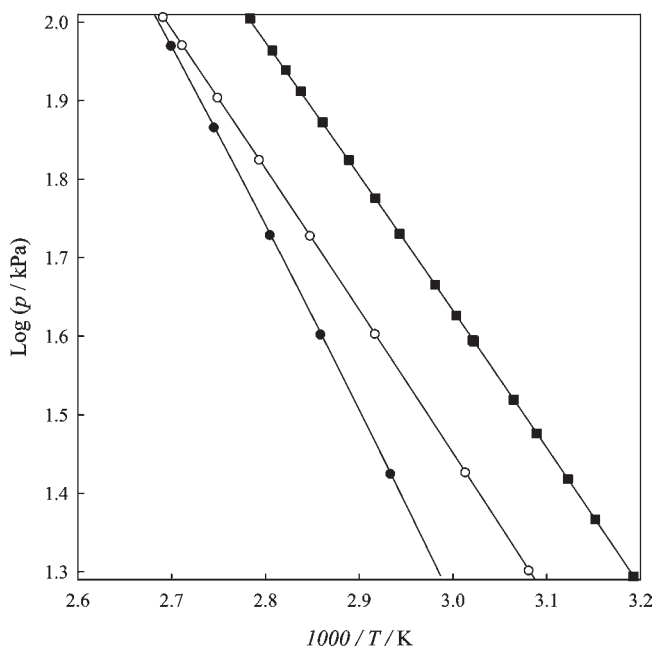


Figure 4. Vapor pressure (p) as a function of temperature (T) for pure fluids. —, predicted by eq 3 and parameters reported in Table 12. Experimental reported data: ●, 2-butanol;³⁷ ○, *n*-heptane;³⁸ ■, TAME.³⁹

Critical properties were taken from Daubert and Danner.³² The molar virial coefficients B_{ii} , B_{jj} and B_{ij} were estimated by the method of Hayden and O'Connell³⁵ using the molecular and solvation parameters η suggested by Prausnitz et al.³⁶ for the case of 2-butanol and *n*-heptane. For the case of TAME, molecular parameters and physical properties were also taken

Table 13. Estimated Azeotropic Coordinates for the Binary Systems^a

2-butanol (1) + <i>n</i> -heptane (2)		
pressure/kPa	x_1^{Az}	T^{Az}/K
50	0.345	341.69
75	0.386	352.67
94	0.409	359.14
2-butanol (1) + TAME (3)		
pressure/kPa	x_1^{Az}	T^{Az}/K
50	0.011	337.64
75	0.062	349.62
94	0.096	356.67

^a T^{Az} is the azeotropic temperature, and x_1^{Az} is the azeotropic mole fraction.

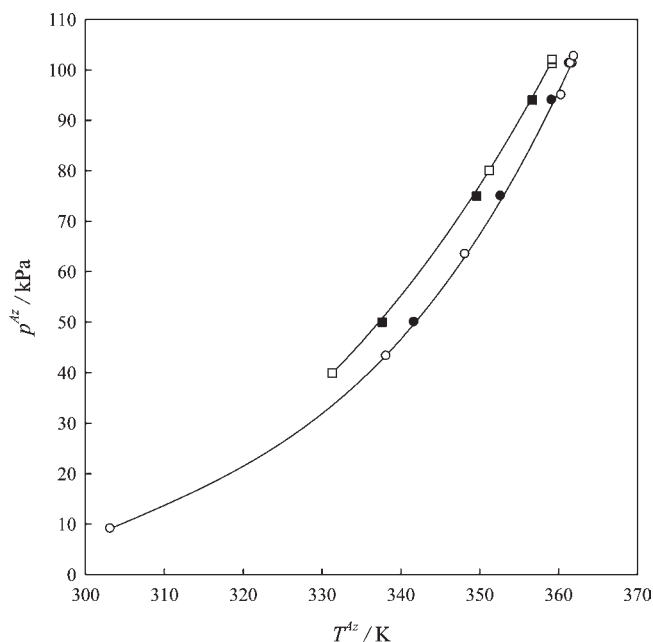


Figure 5. Azeotropic point evolution. 2-Butanol (1) + *n*-heptane (2): ●, this work; ○, data reported in refs 13, 15, 16, 18 to 20, and 40. 2-Butanol (1) + TAME (2): ■, this work; □, data reported in refs 12 and 21.

from ref 32, while the solvation parameter was estimated by smoothing experimental data of second virial coefficients, thus yielding the value $\eta = 0.105$. B_{ii} , B_{jj} and B_{ij} values are reported in Tables 2 to 10.

The vapor pressures of the pure components were also experimentally determined using the same equipment as that for obtaining the VLE data, and experimental values are presented in Table 11. The temperature dependence of the vapor pressure P_i^0 was correlated using the Antoine equation:

$$\log(P_i^0/\text{kPa}) = A_i - \frac{B_i}{(T/K) + C_i} \quad (3)$$

where the Antoine constants A_i , B_i , and C_i are reported in Table 12. Equation 3 correlated the vapor pressure data of the

pure fluids within a maximum absolute percentage deviation (ADP) of 0.30 %. Figure 4 shows a comparison between the vapor pressure predicted from eq 3 with the parameters presented in Table 12 and the experimental data reported by other authors. From this figure it is possible to observe that the Antoine's parameters presented in Table 12 predict very well the experimental vapor pressure data reported by Ambrose

and Sprake³⁷ (ADP = 0.31 %) for 2-butanol, ADP = 0.18 % for *n*-heptane,³⁸ and by Krahenbühl and Gmehling³⁹ (ADP = 0.17 %) for TAME, and confirm the thermometer calibration.

The experimental data reported in Tables 2 to 10 allow concluding that the binary mixtures exhibit positive deviation from ideal behavior and azeotropy is confirmed at (50, 75, and 94) kPa for the case of binary mixtures with 2-butanol. The azeotropic concentrations of the measured binaries with 2-butanol were estimated by fitting the function

$$f(x) = 100 \left(\frac{y-x}{x} \right) \quad (4)$$

where $f(x)$ is an empirical interpolating function and x and y have been taken from the experimental data. Azeotropic concentrations, as determined by solving $f(x) = 0$, are indicated in Table 13. From the latter table we observe that the mole fraction of the azeotrope impoverishes in 2-butanol as pressure (or temperature) increases. The evolution of the azeotropic point agrees well with the results presented by other authors,^{13,15,16,18–20,40} as it is shown in Figure 5.

The VLE data reported in Tables 2 to 10 were found to be thermodynamically consistent by the point-to-point method of Van Ness et al.⁴¹ as modified by Fredenslund et al.⁴² For each isobaric condition, consistency criterion ($\Delta y < 0.01$) was met by fitting the equilibrium vapor pressure of the mixture according to the Barker's⁴³ reduction method. Statistical analysis reveals that a three-parameter Legendre polynomial is adequate for fitting the equilibrium vapor pressure in each case. Pertinent consistency statistics and Legendre polynomial parameters are presented in Table 14.

The VLE data reported in Tables 2 to 10 were correlated with the Wohl, nonrandom two-liquid (NRTL), Wilson, and universal quasichemical (UNIQUAC) equations,⁴⁴ whose adjustable parameters were obtained by minimizing the following objective

Table 14. Consistency Test Statistics for the Binary Systems

2-butanol (1) + <i>n</i> -heptane (2)					
pressure/kPa	L_1^a	L_2^a	L_3^a	$100 \cdot \Delta y^b$	$\delta P^c/\text{kPa}$
50.00	1.6114	-0.2769	0.1353	0.6	0.1
75.00	1.5223	-0.2362	0.0917	0.5	0.2
94.00	1.4770	-0.1985	0.0776	0.3	0.3
2-butanol (1) + TAME (3)					
pressure/kPa	L_1^a	L_2^a	L_3^a	$100 \cdot \Delta y^b$	$\delta P^c/\text{kPa}$
50.00	0.6746	-0.1376	0.0056	0.4	0.1
75.00	0.6421	-0.1189	-0.0318	0.4	0.2
94.00	0.6383	-0.0970	0.0085	0.2	0.3
<i>n</i> -heptane (2) + TAME (3)					
pressure/kPa	L_1^a	L_2^a	L_3^a	$100 \cdot \Delta y^b$	$\delta P^c/\text{kPa}$
50.00	0.1572	-0.0010	0.0000	0.4	0.4
75.00	0.1602	-0.0118	-0.0016	0.4	0.1
94.00	0.1621	-0.0070	-0.0010	0.5	0.1

^a Parameters for the Legendre polynomial (L_1, L_2, L_3)⁴² used in consistency. ^b Average absolute deviation in vapor phase mole fractions $\Delta y = (1/N) \sum_{i=1}^N |y_i^{\text{exptl}} - y_i^{\text{cal}}|$ (N : number of data points). ^c Average absolute deviation in vapor pressure $\delta P = (1/N) \sum_{i=1}^N |P_i^{\text{exptl}} - P_i^{\text{cal}}|$.

Table 15. Parameters and Prediction Statistics for Different Gibbs Excess (G^E) Models in 2-Butanol (1) + *n*-Heptane (2)^a

model	P/kPa	A_{12}	A_{21}	α_{12}	bubble-point pressures		dew-point pressures		γ deviations	
					$\Delta P(\%)^f$	$100 \cdot \Delta y_i^g$	$\Delta P(\%)^f$	$100 \cdot \Delta x_i^g$	$\Delta \gamma_1(\%)^f$	$\Delta \gamma_2(\%)^f$
Wohl	50.00	1.839	1.351	1.365 ^d	0.66	0.8	0.52	1.6	0.07	0.05
	75.00	1.736	1.298	1.337 ^d	0.43	0.6	0.46	1.2	0.07	0.09
	94.00	1.654	1.277	1.297 ^d	0.43	0.6	0.44	1.0	0.10	0.11
NRTL	50.00	1257.81	4172.91	0.3000 ^e	0.66	0.8	0.66	1.5	0.07	0.05
	75.00	1183.72	4114.24	0.3000 ^e	0.45	0.6	0.46	1.1	0.07	0.09
	94.00	1240.49	3921.73	0.3000 ^e	0.47	0.5	0.42	0.9	0.10	0.11
Wilson ^b	50.00	5873.90	474.30		0.34	0.3	0.46	0.5	0.07	0.05
	75.00	5657.14	386.03		0.27	0.3	0.43	0.4	0.07	0.09
	94.00	5422.04	433.80		0.41	0.2	0.41	0.3	0.10	0.11
UNIQUAC ^c	50.00	-835.53	2764.03		0.69	0.8	0.56	1.6	0.07	0.05
	75.00	-870.76	2771.83		0.46	0.7	0.46	1.2	0.07	0.09
	94.00	-847.47	2687.66		0.48	0.6	0.43	1.0	0.10	0.11

^a A_{12} and A_{21} are the G^E model parameters $\text{J} \cdot \text{mol}^{-1}$. ^b Liquid molar volumes have been estimated from the Rackett equation.³⁴ ^c Molecular parameters are those calculated from UNIFAC^{41,45} using the following r and q parameters: $r_1 = 3.3949$, $r_2 = 5.1742$, $q_1 = 3.0160$, $q_2 = 4.3960$. ^d q parameter for the Wohl's model. ^e α_{12} parameter for the NRTL model. ^f $\Delta \sigma = (100/N) \sum_{i=1}^N |\sigma_i^{\text{exp}} - \sigma_i^{\text{cal}}| / \sigma_i^{\text{exp}}$ with $\sigma = P$ or γ . ^g $\Delta \sigma = 1/N \sum_{i=1}^N |\delta_i^{\text{exp}} - \delta_i^{\text{cal}}|$ with $\delta = y$ or x .

Table 16. Parameters and Prediction Statistics for Gibbs Excess (G^E) Models in 2-Butanol (1) + TAME (3)^a

model	P/kPa	A_{12}	A_{21}	α_{12}	bubble-point pressures		dew-point pressures		γ deviations	
					$\Delta P(\%)^f$	$100 \cdot \Delta y_i^g$	$\Delta P(\%)^f$	$100 \cdot \Delta x_i^g$	$\Delta \gamma_1(\%)^f$	$\Delta \gamma_3(\%)^f$
Wohl	50.00	0.816	0.553	1.060 ^d	0.16	0.3	0.31	0.4	0.06	0.06
	75.00	0.771	0.519	0.946 ^d	0.29	0.3	0.39	0.3	0.09	0.06
	94.00	0.756	0.554	1.359 ^d	0.31	0.2	0.29	0.3	0.10	0.06
NRTL	50.00	-520.72	2897.79	0.3000 ^e	0.14	0.4	0.33	0.4	0.06	0.06
	75.00	-622.97	3012.45	0.3000 ^e	0.36	0.3	0.47	0.3	0.09	0.06
	94.00	-335.85	2595.48	0.3000 ^e	0.30	0.3	0.29	0.3	0.10	0.06
Wilson ^b	50.00	3453.86	-1061.16		0.18	0.3	0.38	0.4	0.06	0.06
	75.00	3589.44	-1180.57		0.42	0.3	0.51	0.3	0.09	0.06
	94.00	3327.62	-1027.34		0.32	0.2	0.31	0.3	0.10	0.06
UNIQUAC ^c	50.00	-1161.17	2242.17		0.18	0.3	0.35	0.4	0.06	0.06
	75.00	-1222.06	2325.47		0.35	0.3	0.46	0.3	0.09	0.06
	94.00	-1139.93	2164.24		0.30	0.2	0.28	0.3	0.10	0.06

^a A_{12} and A_{21} are the G^E model parameters $J \cdot \text{mol}^{-1}$. ^b Liquid molar volumes have been estimated from the Rackett equation.³⁴ ^c Molecular parameters are those calculated from UNIFAC^{41,45} using the following r and q parameters: $r_1 = 3.3949$, $r_3 = 4.7422$, $q_1 = 3.0160$, $q_3 = 4.1720$. ^d q parameter for the Wohl's model. ^e α_{12} parameter for the NRTL model. ^f $\Delta \sigma = (100/N) \sum_i^N |\sigma_i^{\text{exp}} - \sigma_i^{\text{cal}}| / \sigma_i^{\text{exp}}$ with $\sigma = P$ or γ . ^g $\Delta \delta = 1/N \sum_i^N |\delta_i^{\text{exp}} - \delta_i^{\text{cal}}|$ with $\delta = y$ or x .

Table 17. Parameters and Prediction Statistics for Different Gibbs Excess (G^E) Models in *n*-Heptane (2) + TAME (3)^a

model	P/kPa	A_{12}	A_{21}	α_{12}	bubble-point pressures		dew-point pressures		γ deviations	
					$\Delta P(\%)^f$	$100 \cdot \Delta y_i^g$	$\Delta P(\%)^f$	$100 \cdot \Delta x_i^g$	$\Delta \gamma_2(\%)^f$	$\Delta \gamma_3(\%)^f$
Wohl	50.00	50.00	0.2053	0.1216	2.3155 ^d	0.14	0.2	0.17	0.04	0.05
	75.00	75.00	0.1999	0.1259	2.0776 ^d	0.19	0.3	0.23	0.10	0.06
	94.00	94.00	0.1947	0.1279	2.1597 ^d	0.24	0.4	0.28	0.10	0.06
NRTL	50.00	50.00	-444.56	980.40	0.3000 ^e	0.10	0.4	0.18	0.04	0.05
	75.00	75.00	-444.07	979.90	0.3000 ^e	0.10	0.4	0.19	0.10	0.06
	94.00	94.00	-443.97	980.21	0.3000 ^e	0.12	0.5	0.17	0.10	0.06
Wilson ^b	50.00	50.00	708.86	-162.74		0.10	0.3	0.16	0.04	0.05
	75.00	75.00	719.53	-155.34		0.10	0.4	0.18	0.10	0.06
	94.00	94.00	722.13	-153.08		0.15	0.4	0.20	0.10	0.06
UNIQUAC ^c	50.00	50.00	-404.09	544.00		0.11	0.3	0.17	0.04	0.05
	75.00	75.00	-402.68	545.70		0.10	0.4	0.18	0.10	0.06
	94.00	94.00	-414.41	558.72		0.14	0.5	0.19	0.10	0.06

^a A_{12} and A_{21} are the G^E model parameters $J \cdot \text{mol}^{-1}$. ^b Liquid molar volumes have been estimated from the Rackett equation.³⁴ ^c Molecular parameters are those calculated from UNIFAC^{41,45} using the following r and q parameters: $r_2 = 5.1742$, $r_3 = 4.7422$, $q_2 = 4.3960$, $q_3 = 4.1720$. ^d q parameter for the Wohl's model. ^e α_{12} parameter for the NRTL model. ^f $\Delta \sigma = (100/N) \sum_i^N |\sigma_i^{\text{exp}} - \sigma_i^{\text{cal}}| / \sigma_i^{\text{exp}}$ with $\sigma = P$ or γ . ^g $\Delta \delta = 1/N \sum_i^N |\delta_i^{\text{exp}} - \delta_i^{\text{cal}}|$ with $\delta = y$ or x .

function (OF):

$$\text{OF} = \sum_{i=1}^N (|P_i^{\text{exp}} - P_i^{\text{cal}}| / P_i^{\text{exp}} + |y_i^{\text{exp}} - y_i^{\text{cal}}|)^2 \quad (5)$$

Pertinent parameters are reported in Tables 15 to 17, together with the relative deviation for the case of bubble- and dew-point pressures. From the results presented in the quoted tables, it is possible to conclude that all of the fitted models gave a reasonable correlation of the binary system; the best fit is obtained with the Wilson model. The capability of predicting simultaneously the bubble- and dew-point pressures and the vapor and liquid

phase mole fractions, respectively, has been used as the ranking factor. To establish the coherency of the present binary data and to test the predictive capability of the parameters reported in Tables 15 to 17, we have used the best-ranked model (Wilson's model) to predict the binary VLE data reported in other sources. For the case of 2-butanol + *n*-heptane, we can observe a good agreement both in the predicted bubble-point ($\Delta P < 5.6\%$, $\Delta y_i < 3.0\%$) and dew-point pressures ($\Delta P < 3.6\%$, $\Delta x_i < 3.9\%$) for the case of isothermal data and a fair good agreement both in the predicted bubble-point ($\Delta T < 1.5\%$, $\Delta y_i < 1.5\%$) and dew-point temperature ($\Delta T < 0.37\%$, $\Delta x_i < 0.8\%$) for the case of isobaric

data. For the case of *n*-heptane + TAME mixture, the parameters reported in Table 17 provide good agreement in the predicted bubble-point ($\Delta T < 0.2\%$, $\Delta y_i < 0.8\%$) and dew-point temperature ($\Delta T < 0.1\%$, $\Delta x_i < 0.8\%$) for the case of isothermal data reported by other authors.^{22–24} In addition to the previous results, Tables 15 to 17 also include the average deviation of the activity coefficients predicted from the GE models using the parameters reported in the quoted tables. As we can observe, the maximum obtained average deviation is 1%. As we can see from the results present here, binary mixtures are well-characterized, and their G^E parameters provide good agreement with previous works.

Finally, we explored the phase behavior of the ternary system (2-butanol (1) + *n*-heptane (2) + TAME (3)), as predicted with the Redlich–Kister expansion⁴⁶ from binary contributions. The binary parameters of the Redlich–Kister were not fitted from binaries but directly transformed from the Legendre polynomial coefficients reported in Table 14. Thus, ternary predictions were reasonably obtained from the same model that was used for analyzing the consistency of the binary data. In the Supporting Information section, we report the numerical value of the binary coefficients for the Redlich–Kister expansion,⁴⁶ as well as the predicted Gibbs excess energy, together with the isobaric phase equilibrium diagrams for the ternary system. The predicted results suggest that the ternary mixture exhibits positive deviations from ideal behavior and, in addition to the azeotropes observed for the binaries composed by 2-butanol, no ternary azeotrope can be observed. We have also detected that the predictions of the NRTL and Wilson models from binary compare well with Redlich–Kister calculations and predict the same features for the ternary system.

CONCLUSIONS

Isobaric VLE data at (50, 75, and 94) kPa have been reported for the binary systems 2-butanol + *n*-heptane, 2-butanol + TAME, and *n*-heptane + TAME. Equilibrium determinations were performed in a VLE still with circulation of both phases. According to experimental results, binary mixtures composed by 2-butanol exhibit positive deviations from ideal behavior, and azeotropy is present over the whole range of experimental determination. The *n*-heptane + TAME system, in turn, exhibits a slight positive deviation from ideal behavior. The activity coefficients and boiling points of these binary mixtures were well correlated using the Wohl, NRTL, Wilson, and UNIQUAC equations, the best fit corresponding to the Wilson model.

ASSOCIATED CONTENT

S Supporting Information. Table S1 summarizes the binary coefficients of the Redlich–Kister expansion used to predict the phase behavior of the ternary system (2-butanol (1) + *n*-heptane (2) + TAME (3)). Figure S1 depicts the excess Gibbs energy for the ternary system at (50, 75, and 94.00) kPa, while Figure S2 illustrates the boiling temperature diagrams for the ternary system at (50, 75, and 94.00) kPa. This material is available free of charge via the Internet at <http://pubs.acs.org>.

AUTHOR INFORMATION

Corresponding Author

*E-mail: amejia@udec.cl and hsejura@udec.cl.

Funding Sources

This work was financed by FONDECYT, Santiago, Chile (Project 1080596).

REFERENCES

- (1) Halim, H.; Ahsraf-Ali, M. *Handbook of MTBE and Other Gasoline Oxygenates*; Marcel Dekker Inc.: New York, 2004.
- (2) Ahmed, F. E. Toxicology and human health effects following exposure to oxygenated or reformulated gasoline. *Toxicol. Lett.* **2001**, *123*, 89–113.
- (3) Bartling, J.; Schloter, M.; Wilke, B. M. Ethyl *tert*-butyl ether (ETBE) and *tert*-amyl methyl ether (TAME) can affect distribution pattern of inorganic N in soil. *Biol. Fertil. Soils* **2010**, *46*, 299–302.
- (4) Zhu, X. L.; Fan, Z. H.; Wu, X. M.; Meng, Q. Y.; Wang, S. W.; Tang, X. G.; Ohman-Strickland, P.; Georgopoulos, P.; Zhang, J. F.; Bonanno, L.; Held, J.; Liou, P. Spatial variation of volatile organic compounds in a “Hot Spot” for air pollution. *Atmos. Environ.* **2008**, *42* (32), 7329–7338.
- (5) Landmeyer, J. E.; Bradley, P. M.; Trego, D. A.; Hale, K. G.; Haas, J. E. MTBE, TBA, and TAME Attenuation in Diverse Hyporheic Zones. *Ground Water* **2010**, *48*, 30–41.
- (6) Komninos, N. P.; Rakopoulos, C. D. Numerical Investigation into the Formation of CO and Oxygenated and Nonoxygenated Hydrocarbon Emissions from Isooctane- and Ethanol-Fueled HCCI Engines. *Energy Fuels* **2010**, *24*, 1655–1667.
- (7) Wallner, T.; Miers, S. A.; McConnell, S. A Comparison of Ethanol and Butanol as Oxygenates Using a Direct-Injection, Spark-Ignition Engine. *J. Eng. Gas Turb. Power, Trans. ASME* **2009**, *131*, 032802.
- (8) Klokova, I. V.; Klimova, T. A.; Emel'yanov, V. E.; Krylov, I. F. Evaluating the efficacy of corrosion inhibitors in automotive gasolines. *Chem. Technol. Fuels Oils* **2005**, *41*, 319–322.
- (9) de Menezes, E. W.; Cataluna, R.; Samios, D.; da Silva, R. Addition of an azeotropic ETBE/ethanol mixture in eurosuper-type gasolines. *Fuel* **2006**, *85*, 2567–2577.
- (10) *Kirk-Othmer Encyclopedia of Chemical Technology*, Vol. 10; John Wiley & Sons: New York, 2001.
- (11) Marsh, K. N.; Niamskul, P.; Gmehling, J.; Böls, R. Review of thermophysical property measurements on mixtures containing MTBE, TAME, and other ethers with non-polar solvents. *Fluid Phase Equilib.* **1999**, *156*, 207–227.
- (12) Gmehling, J.; Böls, R. Azeotropic Data for Binary and Ternary Systems at Moderate Pressures. *J. Chem. Eng. Data* **1996**, *41*, 202–209.
- (13) Vittal Prasad, T. E.; Satyakishore, P.; Ramserish, G. V.; Prasad, D. H. L. Boiling Temperature Measurements on the Binary Mixtures of *n*-Heptane with Some Aliphatic Alcohols. *J. Chem. Eng. Data* **2001**, *46*, 1266–1268.
- (14) Yamamoto, Y.; Maruyama, T. Separating Agents in Azeotropic Distillation of *sec*-Butanol and Water. *Kagaku Kogaku* **1959**, *23*, 635–640.
- (15) Zong, Z.; Zheng, X. A Study on the Phase Equilibria of Alcoholic Solutions (Part Three). *Dalian Gongxueyuan Xuebao* **1981**, *20*, 63–70.
- (16) Sabarathinam, P. L.; Andiappan, A. Prediction of Isobaric Vapor Liquid Equilibria Data from P-t-x Data. Effect of Alcohols on the Separation of Benzene - *n*-Heptane Mixtures. *Indian J. Technol.* **1985**, *23*, 104–108.
- (17) Pierotti, G. J.; Deal, C. H.; Derr, E. L. Activity Coefficients and Molecular Structure. *Ind. Eng. Chem.* **1959**, *51*, 95–102.
- (18) Powell, J. R.; McHale, M. E. R.; Kauppila, A. S.; Acree, M. W. E.; Flanders, P. H.; Varanasi, V. G.; Campbell, S. W. Prediction of anthracene solubility in alcohol + alkane solvent mixtures using binary alcohol + alkane VLE data. Comparison of Kretschmer-Wiebe and mobile order models. *Fluid Phase Equilib.* **1997**, *134*, 185–200.
- (19) Kumar, A.; Katti, S. S. Isothermal Vapor-Liquid Equilibrium of Isomeric Butanols with *n*-Heptane. *Indian J. Technol.* **1980**, *18*, 60–63.

- (20) Kumar, A.; Katti, S. S. Excess Free Energy of Binary Mixtures of Isomeric Butanols with n-Heptane. *Indian J. Chem., Sect. A* **1980**, *19*, 795–797.
- (21) Evans, T. W.; Edlund, K. R. Tertiary Alkyl Ethers. Preparation and Properties. *Ind. Eng. Chem. Ind. Ed.* **1936**, *28*, 1186–1188.
- (22) Moessner, F.; Coto, B.; Pando, C.; Renuncio, J. A. R. Vapor-Liquid Equilibria of Binary Mixtures of n-Heptane with 1,1-Dimethylethyl Methyl Ether and 1,1-Dimethylethyl Methyl Ether. *Ber. Bunsen-Ges. Phys. Chem.* **1997**, *101*, 1146–1153.
- (23) Chamorro, C. R.; Segovia, J. J.; Martin, M. C.; Montero, E. A.; Villamanan, M. A. Phase equilibrium properties of binary and ternary systems containing *tert*-amylmethyl ether (TAME) as oxygenate additive and gasoline substitution hydrocarbons at 313.15 K. *Fluid Phase Equilib.* **1999**, *156*, 73–87.
- (24) Kammerer, K.; Oswald, G.; Rezanowa, E.; Silkenbaeumer, D.; Lichtenthaler, R. N. Thermodynamic excess properties and vapor-liquid equilibria of binary and ternary mixtures containing methanol, *tert*-amyl methyl ether and an alkane. *Fluid Phase Equilib.* **2000**, *167*, 223–241.
- (25) Segura, H.; Mejía, A.; Reich, R.; Wisniak, J.; Loras, S. Isobaric Vapor-Liquid Equilibria and Densities for the System Ethyl 1,1-Dimethylethyl Ether + 2-Propanol. *Phys. Chem. Liq.* **2002**, *40*, 685–702.
- (26) Segura, H.; Mejía, A.; Reich, R.; Wisniak, J.; Loras, S. Isobaric Vapor-Liquid Equilibria and Densities for the Binary Systems Oxolane + Ethyl 1,1-Dimethylethyl Ether, Oxolane + 2-Propanol and Propan-2-One + Trichloromethane. *Phys. Chem. Liq.* **2003**, *41*, 283–301.
- (27) Segura, H.; Mejía, A.; Reich, R.; Wisniak, J.; Loras, S. Isobaric Vapor-Liquid Equilibria for the Ternary System Oxolane + Ethyl 1,1-Dimethylethyl Ether + 2-Propanol at 50 kPa. *Phys. Chem. Liq.* **2003**, *41*, 493–501.
- (28) Mejía, A.; Segura, H.; Cartes, M.; Bustos, P. Vapor-liquid equilibrium, densities, and interfacial tensions for the system ethyl 1,1-dimethylethyl ether (ETBE) + propan-1-ol. *Fluid Phase Equilib.* **2007**, *255*, 121–130.
- (29) Mejía, A.; Segura, H.; Cartes, M.; Calvo, C. Vapor-liquid equilibria and interfacial tensions for the ternary system acetone + 2,2'-oxybis[propane] + cyclohexane and its constituent binary systems. *Fluid Phase Equilib.* **2008**, *270*, 75–86.
- (30) Mejía, A.; Segura, H.; Cartes, M.; Cifuentes, L.; Flores, M. Phase equilibria and interfacial tensions in the systems methyl *tert*-butyl ether + acetone + cyclohexane, methyl *tert*-butyl ether + acetone and methyl *tert*-butyl ether + cyclohexane. *Fluid Phase Equilib.* **2008**, *273*, 68–77.
- (31) Mejía, A.; Segura, H.; Cartes, M. Vapor-liquid equilibria and interfacial tensions of the system ethanol + 2-methoxy-2-methylpropane. *J. Chem. Eng. Data* **2010**, *55*, 428–434.
- (32) Daubert, T. E.; Danner, R. P. Physical and Thermodynamic Properties of Pure Chemicals. *Data Compilation*; Taylor and Francis: Bristol, PA, 1989.
- (33) Van Ness, H. C.; Abbott, M. M. *Classical Thermodynamics of Nonelectrolyte Solutions*; McGraw-Hill Book Co.: New York, 1982.
- (34) Rackett, H. G. Equation of state for saturated liquids. *J. Chem. Eng. Data* **1970**, *15*, 514–517.
- (35) Hayden, J.; O'Connell, J. A generalized method for predicting second virial coefficients. *Ind. Eng. Chem. Process Des. Dev.* **1975**, *14*, 209–216.
- (36) Prausnitz, J. M.; Anderson, T.; Grens, E.; Eckert, C.; Hsieh, R.; O'Connell, J. *Computer Calculations for Multicomponent Vapor-Liquid and Liquid-Liquid Equilibria*; Prentice Hall: New York, 1980.
- (37) Ambrose, D.; Sprake, C. H. S. Vapor Pressure of Alcohols. *J. Chem. Thermodyn.* **1970**, *2*, 631–645.
- (38) *Selected Values of Properties of Hydrocarbons and Related Compounds*, American Petroleum Institute Research Project 44; Thermodynamic Research Center, Texas A&M University: College Station, TX, 1980.
- (39) Krahenbuhl, M. A.; Gmehling, J. Vapor Pressures of Methyl *tert*-Butyl Ether, Ethyl *tert*-Butyl Ether, Isopropyl *tert*-Butyl Ether, *tert*-Amyl Methyl Ether, and *tert*-Amyl Ethyl Ether. *J. Chem. Eng. Data* **1994**, *39*, 759–762.
- (40) Lesteva, T. M.; Budantseva, L. S.; Rogozil'nikova, L. A.; Sokolovskaya, N. V.; Chernaya, V. I. Study of the Formation of Azeotropes that are Formed by Components of the Isoprene Synthesis from 4,4-Dimethyl-1,3-dioxane. *Deposited Doc. VINITI* **1986**, 3615-V86, 1–16.
- (41) Van Ness, H. C.; Byer, S. M.; Gibbs, R. E. Vapor-liquid equilibrium: Part I. An appraisal of data reduction methods. *AIChE J.* **1973**, *19*, 238–244.
- (42) Fredenslund, A.; Gmehling, J.; Rasmussen, P. *Vapor-Liquid Equilibria Using UNIFAC, A Group Contribution Method*; Elsevier: Amsterdam, 1977.
- (43) Barker, J. A. Determination of Activity Coefficients from total pressure measurements. *Aust. J. Chem.* **1953**, *6*, 207–210.
- (44) Prausnitz, J. M.; Lichtenthaler, R. N.; Gomes de Azevedo, E. *Molecular Thermodynamics of Fluid-Phase Equilibria*, 3rd ed.; Prentice-Hall: Upper Saddle River, NJ, 1999.
- (45) Wittig, R.; Lohmann, J.; Gmehling, J. Vapor-Liquid Equilibria by UNIFAC Group Contribution. 6. Revision and Extension. *Ind. Eng. Chem. Res.* **2003**, *42*, 183–188.
- (46) Redlich, O.; Kister, A. T. Thermodynamics of Nonelectrolyte Solutions. *Ind. Eng. Chem.* **1948**, *40*, 341–345.